Article

MODELLING BATHYMETRIC UNCERTAINTY

By R. Hare[1] (Canada), B. Eakins[2] (USA), C. Amante[2] (USA)
1: Canadian Hydrographic Service, Canada
2: University of Colorado, Boulder CO, U.S.A.

Abstract

Modelling depth measurement uncertainty during data collection and processing has become common practice since the release of S-44 4th Edition (IHO, 1998). Hydrographic Offices have also attempted to model uncertainty of legacy bathymetry in order to determine their fitness for various uses. Additional uncertainty can be introduced into representative bathymetry models by various gridding techniques that interpolate depths between measurements. This article reviews sources of measurement uncertainty, looks at methods for estimating uncertainty in legacy data sets and uncertainty that is introduced into bathymetry (digital elevation/depth) models (DEMs/DDMs) by gridding. Applications that could benefit from bathymetric/DEM/DDM uncertainty information include bridge risk management and tsunami inundation modelling.

Keywords: *bathymetry, uncertainty, digital elevation models*

Résumé

La modélisation de l'incertitude des mesures des profondeurs pendant la collecte et le traitement des données est devenue pratique commune depuis la publication de la 4ème Edition de la S-44 (OHI, 1998). Les Services hydrographiques se sont également efforcés de modéliser l'incertitude de la bathymétrie traditionnelle afin de déterminer leur aptitude à différentes utilisations. Une incertitude supplémentaire peut être introduite dans des modèles de bathymétrie représentatifs au moyen de différentes techniques de quadrillage qui interpolent les profondeurs entre les mesurages. Cet article passe en revue les sources d'incertitude dans les mesurages, examine les méthodes d'estimation de l'incertitude dans les ensembles de données traditionnels et l'incertitude introduite dans les modèles d'élévation ou de profondeurs numériques (DEM/DDM) bathymétriques à l'aide du quadrillage. Les applications qui pourraient bénéficier d'informations sur l'incertitude bathymétrique/DEM/DDM incluent la gestion des risques sur la passerelle et la modélisation des inondations en cas de tsunami.

Mots clés : *bathymétrie, incertitude, modèles d'élévation numériques*

Resumen

La modelización de la incertidumbre de las medidas de profundidad durante la recogida y el procesado de datos se ha convertido en una práctica común desde la publicación de la 4ª Edición de la S-44 (OHI, 1998). Los Servicios Hidrográficos han intentado también modelar la incertidumbre de la batimetría tradicional para determinar su idoneidad para varios usos. Puede introducirse una incertidumbre adicional en modelos de batimetría representativos mediante varias técnicas de reticulado que interpolan profundidades entre las medidas. Este artículo revisa las fuentes de incertidumbre en las medidas, estudia métodos para estimar la incertidumbre en las colecciones de datos tradicionales y la incertidumbre que se introduce en modelos de batimetría (elevación digital/profundidad) (DEMs/DDMs) mediante el reticulado. Las aplicaciones que podrían beneficiar de información relativa a una incertidumbre batimétrica/DEM/DDM incluyen la gestión de los riesgos de puente y la modelización de las inundaciones causadas por los tsunamis.

Palabras clave: *batimetría, incertidumbre, modelos de elevación digitales.*

Introduction

The ocean floor is the last great, largely unsurveyed area of Earth. Many coastal areas have not been surveyed for decades, if at all, and the uncertainties in sounding position and depth can be large. Worse, many applications that require accurate depths or shape fidelity of the seafloor, such as tsunami modelling, can magnify errors in underlying bathymetry models.

It has been shown (MacEachren et al., 2005) that decisions made with knowledge of data uncertainty are more effective than decisions made without that knowledge, e.g. for bridge risk management when undertaking passage planning. The same could be said about decisions made using bathymetric uncertainty information when modelling coastal processes.

Measurement uncertainty estimation

Sources of measurement uncertainty

The basic sources of uncertainty for most of today's depth and elevation measurement systems, i.e. single-beam and multibeam sonars, and bathymetric and topographic lidar, are quite well known. There are: sources of uncertainty that contribute only to vertical uncertainty, such as tides, draft and heave; sources of uncertainty that contribute only to horizontal uncertainty, such as horizontal positioning system and heading sensor; and sources of uncertainty that contribute, through some mapping function, to both vertical and horizontal uncertainty, such as range and beam angle uncertainties due to measurement methods and refraction in multibeam echosounding.

Sources of uncertainty can be broken down by:

- Platform:
  static draft, vessel (ship or aircraft) speed, changes in draft with loading and speed changes, location of sensors, vessel dynamics (amount of roll, pitch, heave and yawing);
- Sensor measurements:
  sonar, sound speed profiler (sometimes SVP), roll, pitch, heading, heave and positioning (including horizontal datum);
- Environment:
  tides (including vertical datum), sound speed structure, sea state;
- Integration:
  the time synchronization of all the sensor measurements on a highly dynamic platform; and
- Calibration:
  the misalignment angles between the instrument and the motion sensor, measured during a patch test or other calibration method.

There are still other sources of uncertainty that are more difficult to quantify and are different from the probabilistic forms of measurement uncertainty discussed above. There is uncertainty in what object is actually being detected in each sonar/lidar measurement, such as whether the system detects the actual seafloor or ground surface, or intermediate features such as biological layers, the water surface, suspended sediment, vegetation/tree canopy, etc. Imperfect processing to remove tree canopy and water column returns may leave such objects in the data set. There may also be some uncertainty in the seafloor penetration due to instrument frequency and the acoustic impedance of the materials making up the seabed.

If the instrument beam footprint is larger than the micro-relief of the seabed, e.g. in the case of sand waves, then some averaged value within the beam footprint may be returned. This is especially true in deep water where the sonar beam footprints may cover hundreds of metres. Bathymetric lidar can also suffer from this problem with beam footprints being several metres, whilst topographic lidar footprints are much smaller. Perhaps just as important is the potential failure to survey morphologic features such as pinnacles that may be located between sparse measurements. Such terrain uncertainty occurs where the footprint of the sounding is much smaller than the distance between soundings and is amplified in areas of high rugosity where the wavelength of significant terrain variability is shorter than the measurement spacing.

When it comes to making inter-comparisons between data sets, temporal changes between two survey epochs may play a role in expanding the uncertainty of the differences, especially where the seabed is known to be highly mobile or dynamic (Dorst, 2005). Precise geo-registration of the data sets is also essential, since any uncertainty in the positions in each will contribute to an inflationary uncertainty in the differences. This uncertainty will be further exaggerated over rugged or steeply sloping seabeds.

The surface detection, terrain and temporal change uncertainties mentioned above are not measurement uncertainties, so cannot be estimated by the legacy data techniques described in the next section. They may, however, contribute significantly to derived model uncertainty.

As summarized by the IHO Standards for Hydrographic Surveys, S-44 5th Edition (IHO, 2008), uncertainties associated with the development of the position of an individual (sonar/lidar) beam must include the following:

a) Positioning system uncertainty;
b) Range and beam angle uncertainties;
c) The uncertainty associated with the ray path model (including the sound speed profile for sonars) and the beam pointing angle;
d) The uncertainty in platform heading;
e) System pointing uncertainties resulting from sensor misalignment;

f) Sensor location;
g) Platform motion sensor uncertainties, e.g. roll and pitch;
h) Sensor position offset uncertainties; and
i) Time synchronisation / latency.

Contributing factors to the vertical uncertainty include:

a) Vertical datum uncertainty;
b) Vertical positioning system uncertainties;
c) Water level measurement uncertainties, including co-tidal uncertainties where relevant;
d) Instrument uncertainties;
e) Sound speed uncertainties (for sonars);
f) Ellipsoidal / vertical datum separation model uncertainties;
g) Platform motion uncertainties, i.e. roll, pitch and heave;
h) Vessel draught, settlement and squat (for sonars)
i) Seabed slope (bathymetry systems); and
j) Time synchronisation / latency.

All of these contributing elements can be combined by applying the Law of Propagation of Variances, provided all the assumptions that underpin that law are met. This results in estimates of total propagated uncertainty (TPU) for both the vertical (depth/elevation) component (TPU-V) and its corresponding horizontal position (TPU-H). The precise methodology has been well documented for swath (multibeam) systems (Hare, 1995). The same methodology could easily be applied to lidar data sets, provided a suitable lidar measurement uncertainty model or other estimates were available. The single-beam echosounder TPU can be computed as a special case of the multibeam echosounder, where only the nadir beam is considered.

Estimating uncertainty in legacy data sets

For legacy data, estimating the uncertainty of position and depth may prove somewhat more challenging. One simple way to obtain a crude estimate is by seeking out the standards that were used to classify the survey at the time it was done. The presumption is that the survey met the standards of the day; therefore all the positions and depths must be at least as good as the specification to which they attempted to adhere. But one must use caution, since assuming a particular standard was met can lead to incorrect estimates (Calder, 2006).

Many surveys, in their original form, e.g. fair sheets, field sheets, plans, etc., may have had good metadata as part of their title blocks or reference notes, or recorded in surveys reports. Often, information about position accuracy or method of positioning will be available in the metadata. Typical accuracies for many positioning systems and methods have been tabulated (Hare, 1997) and can be used as a guideline for TPU-H estimation.

The metadata may also include information about the method of depth measurement or the type of echosounder used. These, together with any information about how depths were corrected for tides, draft and other biases or scale factors, may lead to a crude estimation of the TPU-V. The method used in S-44 5th Edition (IHO, 2008) can be applied here, using both fixed (a) and variable (b) contributions to TPU-V as follows:

$$TPU_V = \pm\sqrt{a^2 + (b \times d)^2}$$

where d represents water depth. Note that the coefficients a and b must be the quadratic summation (i.e. the root-sum-square or RSS) of all the contributing fixed and variable uncertainty components respectively.

For analogue survey data, the data may have become digital through table digitization and may have been transformed from other units, e.g. fathoms, and from older datums, e.g. North American Datum of 1927 (NAD 27). Processing errors during these steps may contribute to an expansion of the TPU values estimated above. The process by which this expansion occurs also generally follows the Law of Propagation of Variances. Methods to compute uncertainty contributions from digitization and processing errors can also be found in the literature (Hare, 1997). The method used to combine any number of uncertainty contributions to position is similar to the equation above and is expressed as follows:

$$TPU_H = \pm\sqrt{\sigma_i^2 + \sigma_j^2 + \sigma_k^2 + \ldots}$$

where i, j and k, etc. are the positioning, digitizing and processing errors that contribute to the total propagated horizontal uncertainty.

All of the TPU values discussed above can, of course, be scaled to any confidence interval (C.I.) that is needed (often the 95% C.I. is used) using an appropriate expansion factor. For TPU-V, this is 1.96 for normally distributed univariate errors; for TPU-H, a circular distribution is often adopted, and an expansion factor of 2 is used to obtain a 95% C.I. estimate, where the radius of the circle is often referred to as twice distance root-mean-square, or 2drms. See Calder (2006) for a more detailed approach.

As noted in the first section, older analogue surveys may represent a significant undersampling of the true variability of the seafloor due to the limitations of the map medium and scale, and then-available technologies. Prior to the advent of swath mapping multibeam sonars, single-beam depths were collected under-ship with gaps in the seafloor coverage to the next survey line perhaps including significant, missed seabed-protruding features. For example, dangers to navigation are occasionally discovered in areas where single-beam hydrographic surveys had been conducted in the past. Legacy data may also suffer from a shoal bias, whereby shoal depths were preferentially recorded for charting purposes.

Legacy data also suffer particularly from uncertainty introduced by morphologic change in dynamic areas. While this temporal change uncertainty does not apply to the data at the time of collection, such data being valuable to change analysis, it does contribute to derived model uncertainty where the model may be implied or stated to represent modern morphology.

Model uncertainty estimation

Computer models of bathymetry (digital elevation models or DEMs) represent Earth's solid surface to some varying degree of accuracy. They are used in modelling of ocean processes, coastal and marine spatial planning, ecosystems and habitat research, and hazard mitigation and community planning, especially when integrated with coastal topography.

The models represent, and are derived from, the source measurements. However, they are typically required to be continuous (i.e. a blanket or surface that has no gaps) so that ocean phenomena may be modelled using them. As such, some type of interpolation is often required to estimate depths in areas without measurements. They are often also intended to represent modern bathymetry and may be forced to rely on legacy data in areas without recent surveys.

Individual cells of uniform size and regularly repeating patterns make up the most common type of DEM, with each cell having an assigned elevation value that is expected to be representative of the average elevation of the seafloor or ground surface within the footprint of the cell. Some bathymetry models may use alternative values, such as minimum depth to support safe navigation, while others may depict a particular epoch for documenting coastal change (Buster and Morton, 2011).

The model vertical uncertainty associated with each cell's elevation value depends upon three principal factors (*Figure 1*; Desmet, 1997):

1) the uncertainty of the source measurements, including temporal change uncertainty if data are from different survey epochs;
2) the gridding technique used to build the model and interpolate between measurements; and
3) terrain variability within each cell's footprint, and between measurements.

Model uncertainty is, in turn, propagated into uncertainty in products derived from their use.

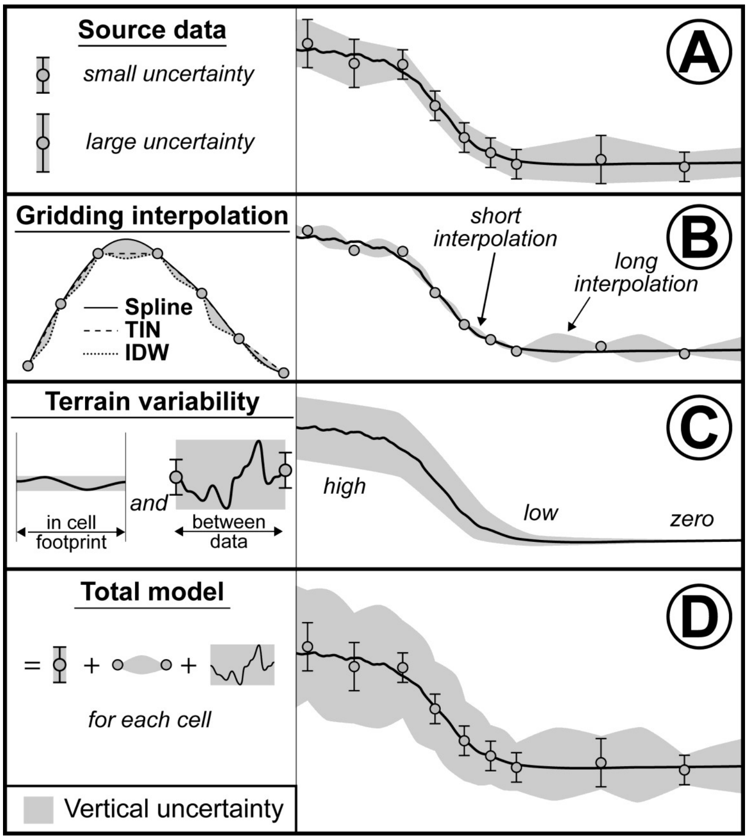

Figure 1 - *Cross-section of factors contributing to each cell's total model vertical uncertainty. A) Source data uncertainty is TPU-V of measurements, as well as temporal change and datum conversion uncertainty. Between data points, the data uncertainty is inferred to be an average of surrounding data uncertainties. B) Gridding interpolation uncertainty grows with distance from source data regardless of technique. It should encompass the range of all possible model surfaces created by various gridding techniques and their adjustable parameters. Gridding uncertainty may be zero in cells constrained by data points if the gridding technique is an exact replicator of source data (e.g. triangulation). C) Terrain variability at wavelengths shorter than the cell footprint or shorter than the distance between measurements contributes additional uncertainty, though it decreases with decreasing variability, potentially reaching zero in flat areas with no variability. D) Total model uncertainty for each cell is the sum of the contributing factors for that cell.*

The primary challenge of integrating bathymetry with topography at the coast, say for modelling inundation from a tsunami or hurricane storm surge, is that bathymetric soundings are typically sparse compared to topographic measurements (e.g. dense lidar surveys may have point spacings of 1 metre or less). The distance between depth measurements may be 10 or 100 times that of land measurements, and even larger far offshore. Development of a model that matches the resolution of topographic data, for detailed inundation mapping, may thus require extreme interpolation of bathymetry (over tens to hundreds of unconstrained model cells). Assessing the uncertainty introduced by gridding techniques when interpolating over such large distances is described in the next section.

Where source bathymetry data are present, the uncertainty associated with each sounding is propagated into the bathymetry model, as is the terrain uncertainty. Where multiple soundings are averaged into a single cell value, as is typically the case with swath data, their individual uncertainties can be combined into the cell data uncertainty. In legacy data, where the soundings may be sparse compared to the bathymetry model's cell size, one sounding may contribute to a single cell. The cell's uncertainty will almost certainly exceed the sounding's uncertainty due to the likely mismatch between footprints of sounding and cell, and to uncertainty contributions from terrain and temporal change, as well as that introduced by the gridding technique.

Finally, because bathymetric and topographic data are typically referenced to different vertical datums, e.g. mean lower low water or North American Vertical Datum of 1988, the data need to be converted to a common vertical datum prior to model development. This vertical datum conversion introduces additional uncertainty into the model.

Uncertainty introduced by gridding techniques

Where no soundings constrain the depth in an individual cell, interpolative gridding is often required to infer the depth based on known surrounding depths; the modelling of ocean processes typically requires each cell to have an elevation value to prevent modelling instabilities. Common gridding techniques include: spline, kriging, inverse distance weighting (IDW), nearest neighbour, and triangulation (Maune et al., 2007). Each technique estimates the depth values using particular constraints, such as a minimum curvature surface for spline, or a linear distance -based weighted average of known soundings for IDW (Burrough and McDonnell, 1998).

DEMs are a model of reality and deviations from the true seabed or land surface constitute errors. DEM errors originate from both the source measurement (e.g. multibeam sonar, lidar) and the interpolative gridding. Guo et al. (2010) found that interpolation errors are as significant as source errors and should be considered when generating and using DEMs. The magnitude of interpolation errors is often unknown and the lack of knowledge about these errors represents the uncertainty introduced by the gridding process (Wechsler, 2007).

Numerous studies indicate that the accuracy of interpolated DEMs is inversely related to terrain complexity (Kubik and Botman 1976; Li, 1992; Gao, 1995; Gong et al., 2000; Erdogan, 2010; Guo et al., 2010). All interpolators are more accurate in areas of low relief as there is a higher degree of spatial dependence between source elevation measurements and the true elevations of nearby unconstrained cells requiring interpolation. In areas of complex terrain, interpolation errors typically increase in magnitude because the true, and unknown, elevation to be interpolated can deviate greatly from nearby source measurements. Consequently, morphometric parameters including slope and curvature can provide insight on the magnitude of interpolation uncertainty. Aguilar et al. (2005) found that the greatest predictor of the accuracy of interpolation was morphology, followed by sampling density and interpolation method. Other studies also indicate that the uncertainty of interpolated elevations increases in areas of heterogeneous terrain and with increasing distance from source measurements (***Figure 2***; Chaplot et al., 2006; Erdogan, 2009).

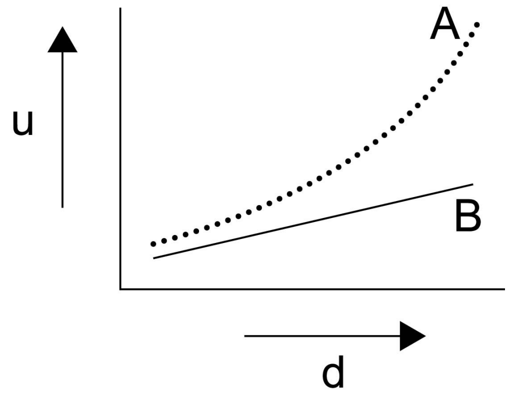

Figure 2 *- Increase in cell elevation uncertainty (u) with interpolation distance (d) from known soundings. Trends A and B may represent either different gridding techniques (e.g., IDW or spline) or areas of different terrain (e.g., smooth/ continental shelf or heterogeneous/submarine canyon).*

In addition, approximate gridding techniques, such as trend surfaces, may force cell values derived from source soundings away from their average elevation value, adding further uncertainty to those cell values. Exact interpolators (e.g. triangulation, IDW) create surfaces that pass exactly through the source data (Desmet, 1997). Gridding techniques may also introduce artefacts into the model, including false oscillations introduced by spline interpolation (Almansa et al., 2002), or "bull's-eye" patterns from IDW interpolation (Gonçalves, 2006).

There are a number of techniques that can be used to quantify the errors of interpolated elevations using known measurements, e.g. split-sample (also referred to as cross-validation), jack-knifing, and boot-strapping (Erdogan, 2009; Paquet, 2010). Using a split-sample approach, a percentage of the data is omitted, an interpolation method is applied, and the differences between the interpolated elevations and the original omitted elevations are calculated (*Figure 3*). In order to quantify the errors of the interpolation method at every data point, this process is repeated and the differences between the original omitted elevations and the interpolated elevations are aggregated. The interpolation errors can be quantitatively assessed by several descriptive statistics including the minimum, maximum, mean, root mean squared error (RMSE), and standard deviation. The split-sample method is often used to assess the stability of various interpolation methods by omitting increasingly greater percentages of the original data and analyzing changes in the interpolation errors (Declercq, 1996; Smith et al., 2005).

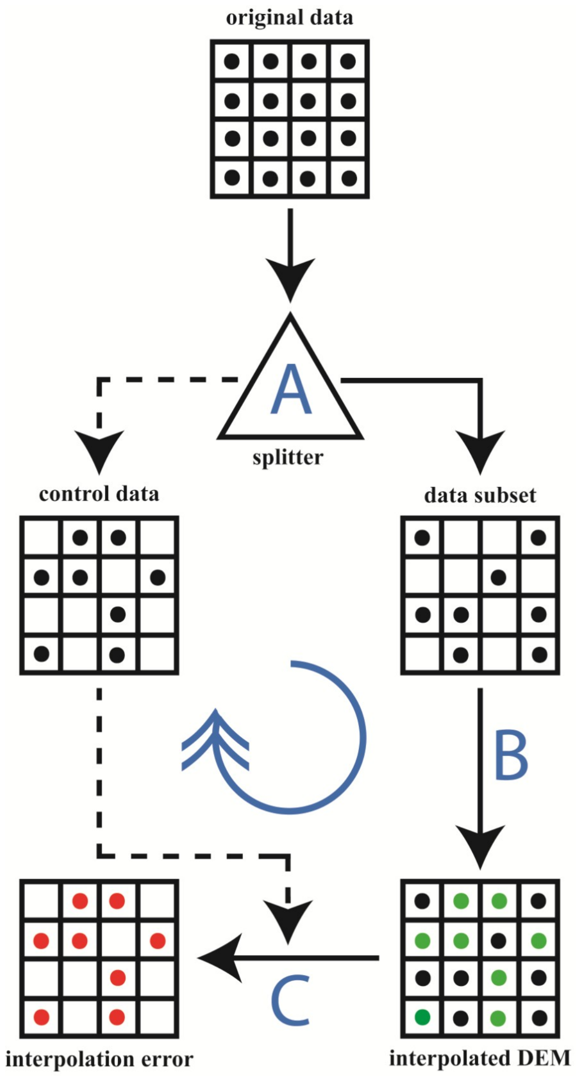

Many studies that quantify interpolation errors using a split-sample approach are based on topography DEMs where dense lidar surveys are reduced by a small percentage (< 10%) and interpolation is only performed over one or a few cells (Hodgson and Bresnahan, 2004; Palamara et al., 2007; Grebby et al., 2010). On the other hand, bathymetry models are often derived from soundings with much greater point spacing, which requires extreme interpolation over tens to hundreds of unconstrained model cells in order to be consistent with the resolution of coastal lidar surveys.

Studies also indicate that statistical measurements, such as RMSE and standard deviation, are insufficient in fully characterizing interpolation errors (Desmet, 1997; Erdogan, 2009). These global descriptive statistics assume uniform values for the entire DEM, which is often not the case (Erdogan, 2009). Consequently, it is also important to investigate the spatial pattern of interpolation errors that result from distance from control points in heterogeneous terrain (Chaplot et al., 2006). The combination of statistical measurements and spatial patterns of interpolation errors is being used in an ongoing research project to quantify the uncertainty introduced by each gridding technique as it relates to distance to control points and surface characteristics such as slope and curvature, quantitative results of which will be published separately.

Figure 3. *Flowchart depicting the split-sample methodology for quantifying interpolation errors. A) The original data are averaged to have exactly one elevation value per grid cell. They are then randomly split by a fixed percentage (e.g., 50%) into control data and data subset. B) An interpolation method (e.g. spline, triangulation, IDW) is applied to the data subset to build an interpolated DEM. C) The interpolated DEM is compared to the control data to quantify the interpolation errors. Steps A to C are repeated at the same split percentage (randomness resulting in different control data and data subset) to determine interpolation error at every grid cell and account for bathymetric variability. The method is rerun iteratively using different split percentages to evaluate the stability (e.g. ability to reproduce the principal topography) of the chosen interpolation method with various data densities.*

Applications for bathymetric DEM with uncertainty

Coastal inundation modelling

A primary use of DEMs that integrate bathymetry and topography is the modelling of coastal inundation from either tsunamis or hurricane storm surges (Eakins and Taylor, 2010). The hydrodynamics of the particular phenomena are modelled upon the DEM, and the location of the resulting maximum inundation line is then used for hazard mitigation planning or operationally during real-time events to help define evacuation areas.

Uncertainty in the cell elevation values directly affects the model hydrodynamics, but they also contribute to horizontal uncertainty of the inundation line. This last piece of information is critical to emergency managers planning for, or responding to, hazard events. The current practice is to assume some additional buffer area beyond the modelled inundation line to use as the basis for decision making. A better practice would be to propagate DEM uncertainty, along with modelling uncertainty into a TPU-H of the inundation line, which would provide more realistic uncertainties on which to base decision making. A recent study by White et al. (2011) used a stochastic (Monte Carlo) approach to estimate the uncertainty of lidar-derived shorelines. Beekhuizen et al. (2011) also used a Monte Carlo approach to quantify the effect of DEM uncertainty on the positional accuracy of airborne imagery. It would be worthwhile to apply a similar methodology to quantify the propagation of DEM uncertainty into storm-surge and tsunami inundation modelling uncertainty.

Bridge risk management

Another application for bathymetry models with uncertainty is for voyage planning and risk management on a ship's bridge. Traditionally, this task has been done using information contained on the paper chart, such as from a source classification diagram (***Figure 4***), reliability diagram or from notes and symbology on the chart itself. The diagrams, when present, are always at a much smaller scale and contained somewhere within the chart limits, but the information about the quality of the data is never coincident with the data itself. While bathymetry uncertainty is not explicitly stated, it could be crudely implied by experienced mariners and hydrographers from the information given in tabular form.

Figure 4:
Example Source Classification Diagram. Areas in the map have labels (letters) that refer to the table where an indication is given of where the source data originated, its resolution (as defined by line spacing usually) and its age.

SOURCE CLASSIFICATION DIAGRAM / DIAGRAMME DE CLASSIFICATION DES SOURCES

Area/Zone	Origin/Origine	Date	Line spacing/Espacement des lignes
a	CHS/SHC	1997-2008	*
b	VFPA	1995,2005	4m
c	CHS/SHC	1985-1990	10m
d	CHS/SHC	2003	12m
e	CHS/SHC	1987	20m
f	CHS/SHC	1963	30m

VFPA – Vancouver Fraser Port Authority
* Full-bottom coverage/entière couverture du fond

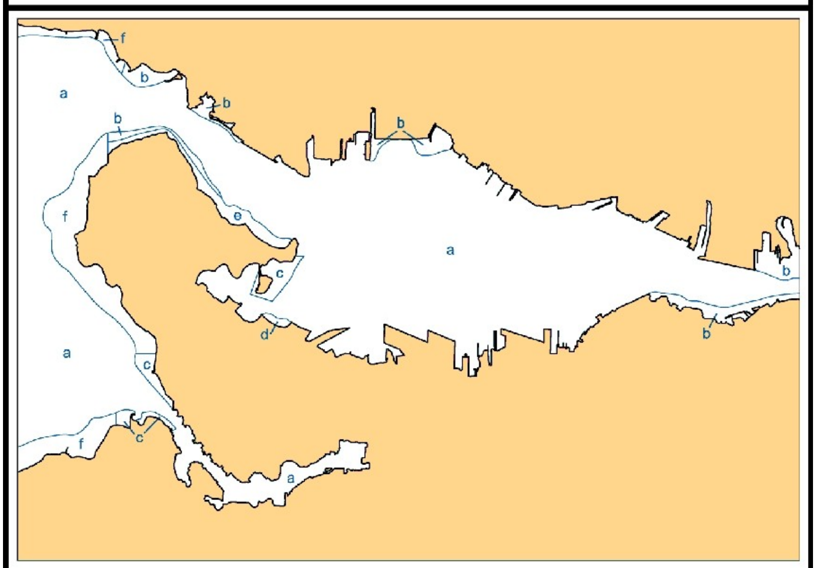

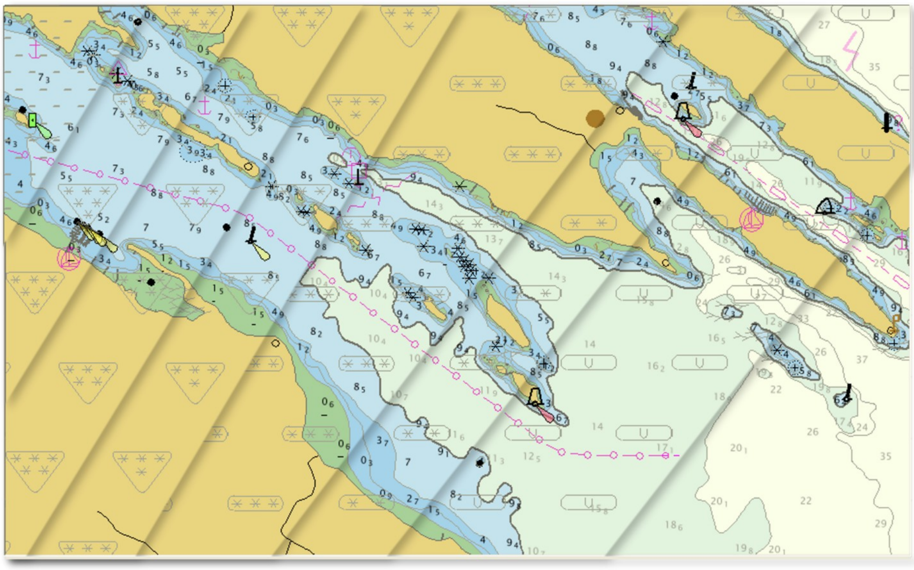

Figure 5 - Example ENC with M_QUAL CATZOC layer turned on. M_QUAL zones of confidence (CATZOCs) are represented by grey stars (*) surrounded by rounded rectangles or inverted rounded triangles, where more stars represents greater confidence that a mariner might put in the data. "U" means unassessed. See Table 1 for further explanation. Note that this is not a real ENC and is for illustrative purposes only. M_QUAL CATZOCs are for bathymetry and would not be coded over land features unless set to unassessed.

More recently, electronic navigational charts (ENCs) have been encoded with a quality metadata layer in the form of zones of confidence, or ZOC. The level of CATZOC, as it is called in the ENC encoding world, can be displayed coincident with the data, allowing decisions to be made with both the data and the uncertainty in context (*Figure 5*).

Still, this is a discrete representation of the uncertainty information (a continuous variable) which may not be particularly helpful or intuitive for the mariner to make informed decisions about the level of risk-taking by navigating in these areas. The CATZOC describes the process by which the data was gathered (what the hydrographer did) rather than what is truly known about the area (what the mariner wants to know). This makes source, reliability and CATZOC diagrams ineffective in conveying the real accuracy of the seabed representation to the end user. The tabular representation of ZOCs is given in ***Table 1***.

Zone of Confidence	Horizontal uncertainty	Vertical uncertainty	Seafloor coverage
A1 *** ** *	± 5m + 5% depth	0.5m + 1% depth	Full area search undertaken. Significant seafloor features detected and measured.
A2 *** **	± 20m	± 1m + 2% depth	Full area search undertaken. Significant seafloor features detected and measured.
B *** *	± 50m	± 1m + 2% depth	Full area search not achieved; uncharted features, hazardous to surface navigation are not expected but may exist.
C ***	± 500m	2m +5% of depth	Full area search not achieved, depth anomalies may be expected.
D **	Worse than ZOC C	Worse than ZOC C	Full area search not achieved, large depth anomalies may be expected.
U	Unassessed – The quality of the bathymetric data has yet to be assessed		
- - -	Unknown (shown for illustrative purposes only; not a legitimate coding)		
	None (illustrates how the ENC would look with CATZOC turned off)		

Table 1 - *Zones of Confidence (ZOC) at the 95% confidence interval (CI). All of these ZOC types are represented in Figure 5 in diagonal bands from the SE corner to the NW corner.*

With the implementation of new standards for encoding data in ENCs, e.g. BAGs (ONSWG, 2006), S-10x product specification (Ward and Greenslade, 2011), etc., it should become possible to see and use the depth DEM and its associated uncertainty estimate DEM in the same electronic chart display (***Figures 6A*** and ***6B*** respectively).

Yet still more powerful is the combination of the two values into a single layer, with the display customized to the draft of the vessel.

An example might be:

- Subtract 2 times the uncertainty from the charted depth (statistically shoal-biasing it at about the 95% C.I.);
- Apply predicted or real-time tides (biased with their 95% uncertainty if available) to charted values to get real-time shoal-biased depths;
- Apply a model of vessel draft variability (biased by the model uncertainty for safety)
- Apply a vessel draft buffer (the captain's comfort zone of clearance beneath the keel);
- Colour-code the resultant depths using:
  - o Green (or no colour at all) – where the shoal-biased, real-time depths exceed the vessel draft plus draft buffer (a safe-to-go zone);
  - o Yellow – where the biased depths exceed the vessel draft, but the buffer is excluded (a cautionary zone); and
  - o Red – where depths are not sufficient to navigate the vessel under any circumstance, given the present state of the tide (a no-go zone).

This scenario leads to the traffic-light display shown in ***Figure 6C***. Working groups of the IHO are presently investigating other options for displaying data quality information to the mariner for more informed decision making, in preparation for the release of S-101 in 2012.

National survey planning

Knowledge of bathymetry DEM uncertainty can also be used by hydrographic offices (HOs) as a tool for prioritizing work. The Canadian Hydrographic Service (CHS) developed a risk-classification model (Mortimer, 2002) for its entire catalogue of charts (some 950) in order to prioritize charting work in a fiscal environment of dwindling resources. This model was based, inter alia, on the types and frequency of vessel traffic, the depth of water, the complexity of the areas and on records of accidents and incidents in the area. The report also recommended that CHS apply risk-management approaches to its other planning activities.

One can conceive of using a regional or nation-wide DEM of depths with their associated uncertainty estimates in the development of a national survey plan. Areas where the estimated depth, less its estimated uncertainty, is shallower than the draft of expected (or forecast) vessel traffic (with a built-in safety margin) would get the highest priority for resurvey. Of course, uncertainty estimates would have to also consider the age of the data and the dynamic variability of the seafloor when planning a resurvey frequency (Dorst, 2005) in order to optimize use of scarce survey resources.

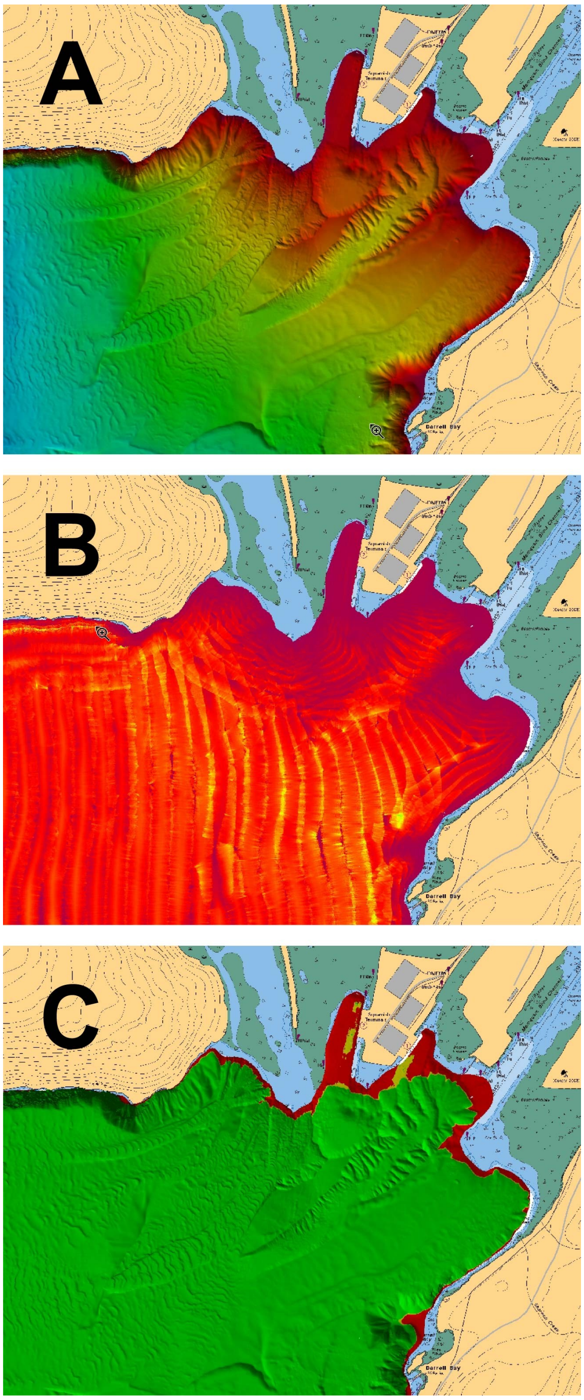

Figure 6. *Example of depth (A) and uncertainty (B) of a bathymetry model viewed within an Electronic Chart display. A "traffic light" display showing "Go" (green), "No-Go" (red) and "Cautionary" (yellow) zones is shown in C. Note: this is only a representation of the uncertainty in the bathymetry; uncertainty in other charted data types that may affect navigation decisions has not been represented.*

If appropriately modelled in a GIS, this national planning model could be re-run at regular intervals (e.g. annually) or each time major changes occur (e.g. due to storms or tsunamis) or when changes are proposed to navigation routes and port facilities.

Summary and conclusions

We have shown the steps involved in estimating bathymetric uncertainty of the source measurements and also those uncertainties due to digitization processes and gridding techniques. Additional sources of uncertainty, such as surface detection, terrain and temporal change may also contribute to the total uncertainty. In addition, we have shown several applications for a terrain model with associated uncertainty, including bridge risk management and tsunami inundation modelling.

There is certainly the potential for myriad applications of a DEM with associated vertical uncertainty estimates. Of the applications examined herein, more work needs to be done on modelling the bathymetric uncertainty over large areas of coastal and offshore North America to support safer marine navigation and hazard preparedness.

Acknowledgments

The initial stimulus for this paper was a request from the NOAA National Geophysical Data Center (NGDC) to CHS for bathymetry data of the west coast of Canada, in order to improve integrated bathymetric-topographic digital elevation models (DEMs) of the west coast of North America to improve tsunami run-up modelling and forecast and warning products. An additional stimulus came from one author's work on the IHO Data Quality Working Group (DQWG), which is presently looking at ways to present uncertainty information about bathymetry to mariners in a more intuitive way. This paper is an update to a paper first presented at US Hydro 2011 in Tampa, Florida, with kind permission of The Hydrographic Society of America (THSOA). Excellent reviewer feedback helped to improve this paper.

References

Aguilar, F.J., Agüera, F., Aguilar, M.A., Carvajal, F. (2005) Effects of terrain morphology, sampling density, and interpolation methods on grid DEM accuracy. *Photogrammetric Engineering and Remote Sensing*, 71, 805–816.

Almansa, A., F. Cao, Y. Gousseau, and B. Rouge. (2002). Interpolation of digital elevation models using AMLE and related methods. *IEEE Transactions on Geoscience and Remote Sensing* 40 (2): 314-25.

Beekhuizen, J., Heuvelink, G.B.M., Biesemans, J., Reusen, I. (2011) Effect of DEM uncertainty on the positional accuracy of airborne imagery. *IEEE Transactions on Geoscience and Remote Sensing*, 49 (5): 1567-1577

Burrough, P.A. and R.A. McDonnell (1998). *Principles of Geographical Information Systems*. Oxford University Press, Oxford.

Buster, N.A., and R.A. Morton (2011) Historical bathymetry and bathymetric change in the Mississippi-Alabama coastal region, 1847–2009. *U.S. Geological Survey Scientific Investigations Map 3154*, 1 sheet, 13-p. pamphlet.

Calder B. (2006) On the uncertainty of Archive Hydrographic Data Sets. *IEEE Journal of Oceanic Engineering,* Vol. 31, No. 2, April 2006, pp. 249-265

Chaplot V., Darboux F., Bourennane H., Leguedois S., Silvera N. & Phachomphon K. (2006) Accuracy of interpolation techniques for the derivation of the digital elevation models in relation to landform types and data density, *Geomorphology,* 77, 126– 141.

Declercq, F.A.N. (1996) Interpolation methods for scattered sample data: accuracy, spatial patterns, processing time. *Cartography and Geographical Information Systems,* 23(3): 128–44.

Desmet, P.J.J. (1997) Effects of interpolation errors on the analysis of DEMs. *Earth Surface Processes and Landforms,* 22, 563–80.

Dorst, L.L. (2005) Optimization of Survey Frequency: The Netherlands Hydrographic Service. *HYDRO International*, Vol. 9, No. 8, October 2005. pp. 6-9.

Eakins B.W. & Taylor L.A. (2010) Seamlessly integrating bathymetric and topographic data to support tsunami modeling and forecasting efforts. *Ocean Globe*, ed. by J. Bremen, ESRI Press, Redlands, CA. pp. 37–56.

Erdogan S. (2009) A comparison of interpolation methods for producing digital elevation models at the field scale. *Earth Surface Processes and Landforms,* 34, pp. 366–376.

Erdogan S. (2010) Modelling the spatial distribution of DEM error with geographically weighted regression: An experimental study. *Computers and Geosciences, 36*, pp. 34-43.

Gonçalves G. (2006) Analysis of Interpolation Errors in Urban Digital Surface Models Created from Lidar Data, *7th International Symposium on Spatial Accuracy Assessment in Natural Resources and Environmental Sciences*, ed. M. Caetano and M. Painho. pp. 160–168.

Gao, J. (1995) Comparison of sampling schemes in constructing DTMs from topographic maps. *ITC Journal*, 1, 18–22.

Gong, J., Li, Z., Zhu, Q., Sui, H. and Zhou, Y. (2000) Effects of various factors on the accuracy of DEMs: an intensive experimental investigation. *Photogrammetric Engineering and Remote Sensing*, 66, 1113–17.

Grebby S., Cunningham D., Naden J. & Tansey K. (2010) Lithological mapping of the Troodos ophiolite, Cyprus, using airborne LiDAR topographic data. *Remote Sensing of Environment, 114*, 713–724.

Guo, Q., Li, W., Yu, H., Alvarez, O. (2010) Effects of topographic variability and lidar sampling density on several DEM interpolation methods. *Photogrammetric Engineering & Remote Sensing*, 76, 1-12.

Hare R.M. (1995) Depth and position error budgets for multibeam echosounding, *International Hydrographic Review*, Monaco, LXXII(2), September 1995, pp. 37-69.

Hare R.M. (1997) *Procedures for Evaluating and Reporting Hydrographic Data Quality*, Internal report, Canadian Hydrographic Service, Department of Fisheries and Oceans.

Hodgson M. E. & Bresnahan P. (2004) Accuracy of airborne lidar-derived elevation: Empirical assessment and error budget. *Photogrammetric Engineering and Remote Sensing*, 70, 331–339.

International Hydrographic Organization (IHO), (1998) *IHO Standards for Hydrographic Surveys, 4th Edition, Special Publication No. 44 (S-44)*, International Hydrographic Bureau, 23 pp.

International Hydrographic Organization (IHO). (2008) *IHO Standards for Hydrographic Surveys, 5th Edition, Special Publication No. 44 (S-44)*, International Hydrographic Bureau, 27 pp.

Li, Z. (1992) Variation of the accuracy of digital terrain models with sampling interval. *Photogrammetric Record*, 14, 113–128.

Kubik, K. And Botman, A.G. (1976) Interpolation accuracy for topographic and geological surfaces. *ITC Journal*, 2, 236 – 274.

MacEachren A.M., Robinson A., Hopper S., Gardner S., Murray R., Gahegan M. & Hetzler E. (2005) Visualizing Geospatial Information Uncertainty: What we know and what we need to know. *Cartography and Geographic Information Science*, Vol. 32, No. 3, pp. 139-160.

Maune D. F., Kopp S.M., Crawford C.A. & Zervas C.E. (2007) Introduction, in *Digital Elevation Model Techniques and Applications: The DEM Users Manual.* 2nd Ed., ed. by D. F. Maune, American Society for Photogrammetry and Remote Sensing, Bethesda, 1–35.

Mortimer A.R. (2002) *A risk-oriented classification of nautical charts*. A report to the Canadian Hydrographic Service. Contract FP802-0-1-0012.

ONSWG. (2006). Open Navigation Surface Working Group. *Format Specification Document: Description of Bathymetric Attributed Grid Object (BAG),* Version 1.0.0. Viewed 08 March 2011. http://www.opennavsurf.org/papers/ons_fsd.pdf

Palamara D. R., Nicholson M., Flentje P., Baafi E. & Brassington G. M. (2007) An evaluation of airborne laser scan data for coalmine subsidence mapping. *International Journal of Remote Sensing,* 28, 3181−3203.

Paquet R. (2010) Estimation of interpolation error in DEMs using statistical methods. *FIG Congress 2010. Facing the Challenges – Building the Capacity*. Sydney, Australia, 11-16 April 2010.

Smith S.L., Holland D.A. & Longley P.A. (2005) Quantifying interpolation errors in urban airborne laser scanning models. *Geographical Analysis,* 37(2): 200–224.

Ward R. & Greenslade B. (2011) "IHO S-100: The Universal Hydrographic Data Model." Viewed 08 March 2011. http://www.iho-ohi.net/mtg_docs/com_wg/TSMAD/TSMAD_Misc/S-100InfoPaper_FinalJan2011.pdf

Wechsler S. (2007) Uncertainties associated with digital elevation models for hydrologic applications: a review. *Hydrology and Earth System Sciences,* 11, 1481–1500.

White, S. A., C. E. Parrish, B. Calder, S. Pe'eri, and Y. Rzhanov. (2011) Lidar-derived national shoreline: empirical and stochastic uncertainty analyses. *Journal of Coastal Research*, Special Issue No. 62, 62-74

Biographies of the authors

Rob Hare is a Manager with Canadian Hydrographic Service. He has worked as a hydrographer and geomatics engineer with CHS since 1982. He is author of numerous papers and reports on hydrographic uncertainty and is Canada's representative on the IHO working group on Standards for Hydrographic Surveys (S-44) and on the IHO Data Quality Working Group (DQWG). (Rob.Hare@dfo-mpo.gc.ca)

Barry Eakins is a marine geophysicist and Scientific Lead for the Marine Geology and Geophysics Division and the Coastal Science Team at NGDC, collaborating through the Cooperative Institute for Research in Environmental Sciences (CIRES), University of Colorado at Boulder (CU). His current research efforts focus on the development of high-resolution digital elevation models that integrate coastal bathymetric and topographic data, in support of tsunami inundation modeling for select U.S. coastal regions. He served 6 years in the U.S. Navy, specializing in oceanography and anti-submarine warfare, before obtaining his B.A. in Geology from CU and his Ph.D. in Earth Sciences from Scripps Institution of Oceanography, University of California, San Diego. (Barry.Eakins@colorado.edu)

Christopher Amante is a professional research assistant collaborating with NGDC through the Cooperative Institute for Research in Environmental Sciences (CIRES) of the University of Colorado at Boulder. Mr. Amante is currently pursuing his Master's degree in Geography from the University of Colorado at Boulder. His research is on the impacts of various gridding

techniques on digital elevation models and tsunami inundation models. He received his B.A. in Environmental Studies with a minor in Physics from the College of the Holy Cross, Worcester, MA.
(Christopher.Amante@colorado.edu)